I-1. PROJECT RESEARCHES

Project 6

PR6

Development on Neutron Imaging Application

Y. Saito

Institute for Integrated Radiation and Nuclear Science, Kyoto University

OBJECTIVES and ALLOTED RESEARCH SUBJECT: Neutron imaging provides valuable information which cannot be obtained from an optical or X-ray imaging. The purpose of this project is to develop the imaging method itself and the experimental environment for expanding the application area of the neutron imaging. The allotted research subjects are as follows:

ARS-1: Measurements of Multiphase Dynamics by Neutron Radiography (Y. Saito et al.)
ARS-2: Effect of Gravity on Void Fraction of Refrigerant Two-Phase Flows in Mini-channels (H. Asano et al.)
ARS-3: Quality visualization of top flooding phenomena in vertical hole (H. Umekawa et al.)
ARS-4: Evaluation of Meltwater Penetration During Defrosting Process (R. Matsumoto et al.)
ARS-5: Spalling Phenomenon of High-Strength Concrete with Different Admixtures (M. Kanematsu et al.)
ARS-6: Neutron Radiography on a 1/16-inch Tee-Shaped Mixer with an Inner Diameter of 1.3 mm Used in Supercritical Hydrothermal Reactor (S. Takami et al.)
ARS-7: Visibility of Plant Roots in Different Artificial Soils via Neutron Imaging (U. Matsushima et al.)
ARS-8: In-situ Observation of Lithium Migration in the Lithium-ion Conductor through Neutron Radiography under High-Temperature (S. Takai et al.)
ARS-9: Measurement of coolant distribution in a flat laminate vapor chamber utilizing neutron radiography (Mizuta et al.)

MAIN RESULTS AND THE CONTENTS OF THIS REPORT:

ARS-1 performed visualization of boiling two-phase flow by high-speed imaging. This study aims to investigate the dynamics of boiling two-phase flow in a heated pipe using high-speed NRG and to clarify the temporal fluctuations.

ARS-2 applied to neutron imaging to void fraction measurements of two-phase flow in a small diameter tube. From measurement results, it was found that the image blur was caused by the beam divergence, resulting in a positive liquid thickness even in the range outside the tube.

ARS-3 investigated the quenching phenomena. Experimental results show the effect of test section geometry on the cooling behavior, including the counter current flow limitation (CCFL).

ARS-4 evaluates the meltwater penetration during defrosting process, which is one of the important phenomena to enhance the energy efficiency of the air conditioning system.

ARS-5 investigates the effect of admixtures in high strength concrete on the spalling phenomenon.

ARS-6 proposed a mixer for the instantaneous heating of the reactant solution and performed neutron radiography measurements. In this study, they tried to visualize the mixing behavior at a teeshaped mixer with an inner diameter of 1.3 mm.

ARS-7 compared the visibility of the root systems of plants cultivated in rice husks and perlite mixed media using neutron imaging.

ARS-8 applies the electric field to the model cell to observe the lithium migration in the solid electrolyte employing the NR.

ARS-9 investigated the change in coolant distribution in a flat vapor chamber with heat input by utilizing neutron radiography.

PR6-1

Measurements of multiphase flow dynamics using neutron radiography

Y. Saito, D. Ito and N. Odaira

Institute for Integrated Radiation and Nuclear Science, Kyoto University

INTRODUCTION: Neutron radiography (NRG) is useful for understanding multiphase flow phenomena. NRG proves effective in understanding thermal-hydraulic phenomena in metallic pipes due to its high transmissivity and has been applied in various applications. It can also measure the flow structure of boiling two-phase flow. Umekawa et al. measured the time-averaged void fraction distribution of boiling two-phase flow under the fluctuated flow rate condition by neutron radiography [1]. This study aims to investigate the dynamics of boiling two-phase flow in a heated pipe using high-speed NRG and to clarify the temporal fluctuations.

EXPERIMENTS: Neutron imaging experiments were conducted in the B-4 facility of KUR. A high-speed imaging system comprising an optical image intensifier and a high-speed camera was employed to acquire sequences of neutron transmission images of boiling flow at 1000 fps. A stainless steel tube with an inner diameter of 6 mm is used as a test section. The test section is heated by Joule heating using a DC power supply whose output can be controlled by the external signal from a function generator. The cross-sectional average void fraction was calculated from the instantaneous void fraction distribution estimated from the transmission images. The dynamics of the flow pattern in the tube were analyzed based on its spatio-temporal distribution.

RESULTS: The spatio-temporal void fraction distributions of boiling flow are shown in Fig.1. The horizontal axis denotes the time and vertical axis denotes the axial distance in the heated tube. The color map represents the cross-sectional averaged void fraction. At the constant heat flux, the generation of vapor bubbles near the center of the imaging area can be confirmed, as shown in Fig.1A. When the test section is heated by sinusoidal power, the distribution shows the fluctuated behavior, as shown in Fig.1B. The position of bubble generation moves in the axial direction as the heat flux changes. The high-speed NRG can measure changes in flow structure in opaque metal pipes and is an effective method for understanding the phenomena of boiling two-phase flow.

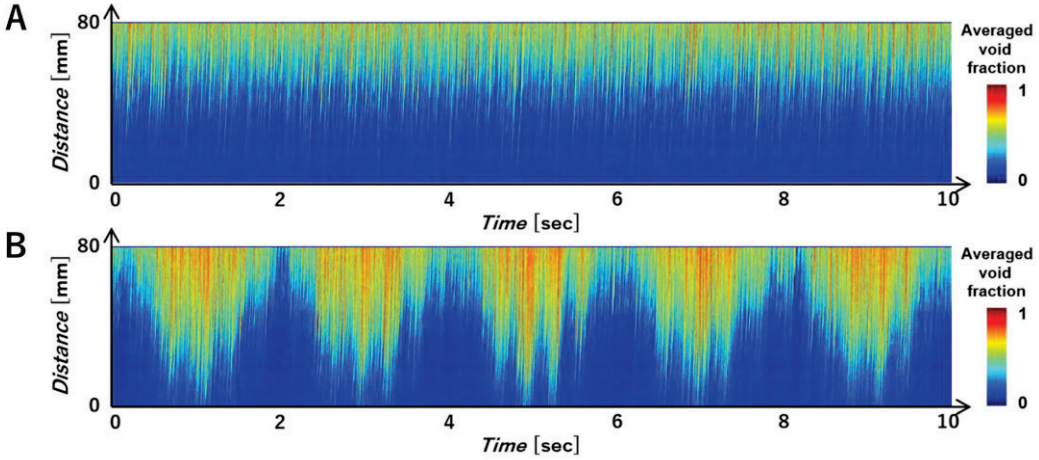

Fig.1. Spatio-temporal distribution of cross-sectional void fraction of constant heat flux of 830 kW/m^2 (A) and fluctuated heat flux with the frequency of 0.5 Hz, the amplitude of 390 kW/m^2 (B).

REFERENCES:

[1] H. Umekawa *et al.,* Physics Procedia, **43** (2013) 269-276.

PR6-2

Effect of Gravity on Void Fraction of Refrigerant Two-Phase Flows in Mini-channels

H. Asano, T. Maruyama, S. Saeki, K. Sugimoto, N. Yoshida, H. Murakawa, Y. Obayashi, K. Nakagawa, Y. Shirase[1], C. Schreiber[1], E. Dzramado[1], J. Inukai[1], N. Odaira[2], D. Ito[2] and Y. Saito[2]

Graduate School of Engineering, Kobe University
[1]Hydrogen and Fuel Cell Nanomaterials Center, University of Yamanashi
[2]Institute for Integrated Radiation and Nuclear Science, Kyoto University

INTRODUCTION: Low-GWP refrigerants are being considered to address the global warming issue, and hydrocarbon-based refrigerants, which are highly flammable natural refrigerants, are also considered as candidates. To apply hydrocarbons to heat pump system, a compact heat exchanger with mini-channels is essential to reduce the refrigerant charge and to improve the coefficient of performance. In this study, the effect of gravity on the void fraction in a mini-channel with an inner diameter of 1 mm, assuming a layered microchannel heat exchanger.

EXPERIMENTS: The test section was a SUS tube with the inner diameter of 1.0 mm and the thickness of 0.5 mm. R134a was used as the working fluid. Gas-liquid two-phase flow was supplied to the test section as a vertical upward flow from a steam generator installed vertically. Horizontal and vertically downward flows were supplied through a bend tube. An example of neutron radiograph is shown in Fig. 1. The tube was filled with liquid. The rectangular area in Fig. 1 shows the measurement area of void fraction. The distance from the entrance to the center of the measurement area is 167, 48, and 52 mm for vertically upward, horizontal and vertically downward flows, respectively. Pixel size was 12.7 μm/pixel with an exposure time of 30 s. The experiment was conducted with mass fluxes of 230, 300, and 400 kg/(m^{2}s) and varied vapor quality from 0.1 to 0.9. The saturation temperature was maintained at 20°C. The bond number, defined as the ratio of the inertia force to the surface tension, was approximately 1.35.

RESULTS: Liquid thickness along the neutron beam direction can be measured by comparison with the image with vapor single-phase at each pixel. Values corresponding to the liquid film thickness for the vertically downward flows are plotted against the distance from the center of the tube as shown in Fig. 2. The vertical axis shows the product of attenuation coefficient of liquid R134a and its thickness in arbitrary unit. The result for liquid single-phase flow represents the cross-sectional shape of the tube. It can be seen from the results that the liquid thickness was positive even in the range outside the tube. The reason is caused by blur due to due to non-parallelism of the neutron beams and the effect of neutron scattering in the object. To measure the cross-section occupied by liquid, it is necessary to integrate the liquid thickness over the area affected, including outside the tube. It was found that the difference in liquid distribution between vertically upward and downward was little.

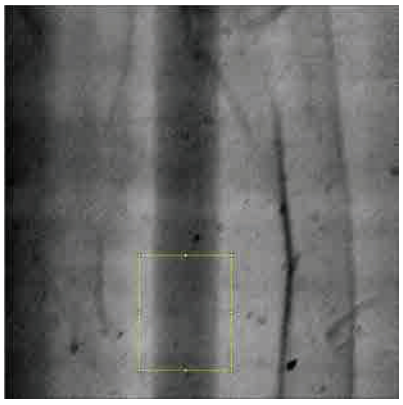

Fig. 1. Neutron radiograph take with reactor thermal out ut 5 MW.

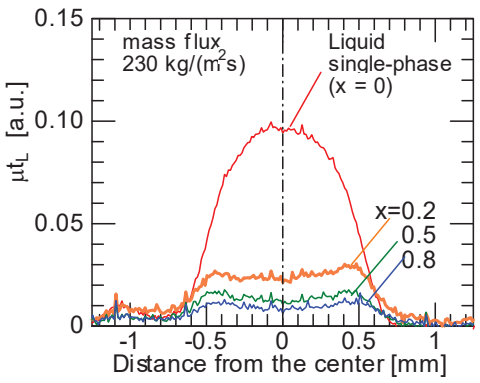

Fig. 2. Radial distribution of liqui thickness along neutron beam.

PR6-3

Qualitatively Visualization of Top Flooding Phenomena in Vertical Hole

H. Umekawa, T. Ami, A. Nanno, K. Inou, Y. Saito[1], D. Ito[1] and N.Odaira. [1]

Department of Mechanical Engineering, Kansai University
[1]Institute for Integrated Radiation and Nuclear Science, Kyoto University

INTRODUCTION: The continuous supply of cold water to a hot surface is a critical factor in the effective cooling of high temperature structures. These phenomena are commonly encountered across various industrial processes and accidents. Typical limitation of cooling process is caused by counter-current flow condition (CCFL) and film boiling. In this investigation, the flow behavior of the cooling water inside a vertical heated tube was qualitatively visualized.

EXPERIMENTS: In this investigation, the test section was initially heated by installing into the electric furnace. Once the temperature of the test section reached the predetermined level, the test section was removed from the furnace, and the cooling water is supplied as the top flooding configuration. During the visualization, the movement of the cooling water was continuously recorded by using highs speed camera. In this term, three kind of test sections was employed, i.e. two round tube (I.D.=3mm and I.D.=8mm, both with t=1mm) and one rectangular tube (I.D.2mm×10mm with t=2mm). The length of these test sections was 75mm, with a closed bottom end, and the top end connected to a water receiver.

Results:

Figure 1 shows the time-strip images of each test sections. These visualization image clearly visualized the influence of the tube geometry. In the case of the large diameter tube (I.D.=8mm), the cooling water reached the bottom end of the tube and periodical cooling behavior was observed. On the other hand, in the case of the small diameter tube (I.D.=3mm) the water could not reach the bottom and mostly stagnated near the entrance part owing to the CCFL condition. In the case of the rectangular tube, water movement expresses the more complex tendency, owing to the separating of the vapor flow and liquid flow at the entrance part. Overall, this visualization in this term, the fundamental procedure can be established, and these results can be utilized in the subsequent detail measurements.

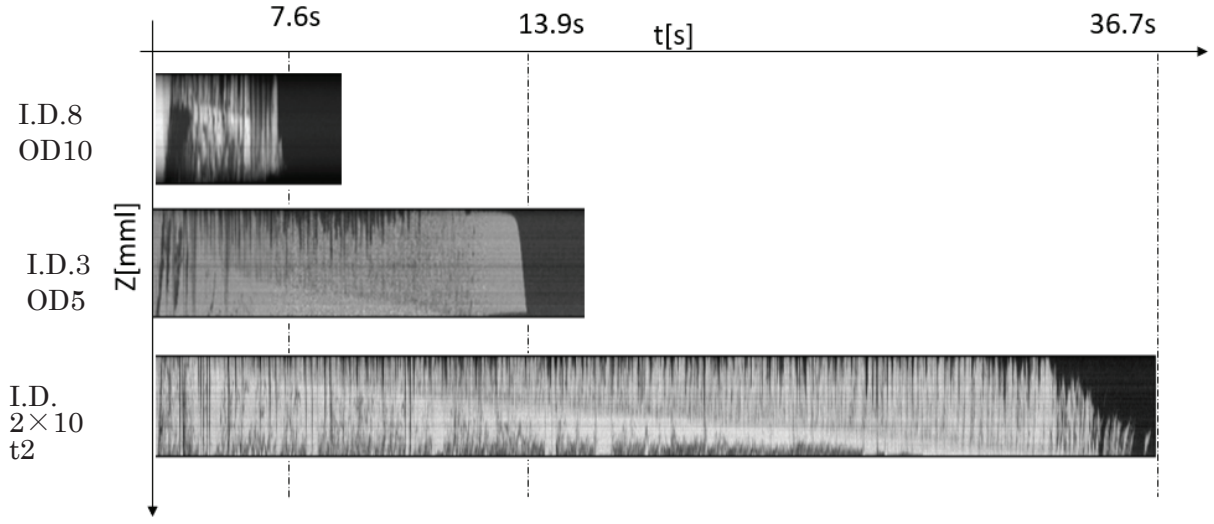

Fig.1 The comparison of time strip image of each test sections.

PR6-4

Evaluation of Meltwater Penetration During Defrosting Process

N. Fujikawa , Q. Chu , R. Matsumoto , S. Kimura , K. Munekiyo , Y. Saito[1] D. Ito[1] and N. Odai-ra[1]

Department of Mechanical Engineering, Kansai Universit
[1]Institute for Integrated Radiation and Nuclear Science, Kyoto University

INTRODUCTION: Frost formation on the heat exchangers of the air conditioning system causes the serious problem on the heat transfer performance. In order to recover the performance of the heat exchanger, a defrosting operation is performed periodically to remove the frost from the heat exchanger. Matsumoto et al. [1] reported the removal of meltwater by penetrating into the remaining frost layer. By using this phenomenon, effective defrosting can be achieved. However, the meltwater penetration mechanism and temperature distribution along the frost layer remain unclear. This study evaluates meltwater penetration behavior using neutron radiography.

EXPERIMENTS AND RESULTS: Frost was formed on the aluminum plate with a thickness of 0.5 mm by cooling it down to -25 °C. A temperature gradient was applied by raising the temperature at one edge of the plate to 1°C, thus, the defrosting was performed in one direction. The defrosting duration was 10 min. The water penetration image at 3 min after the start of defrosting is shown in Fig.1, where defrosting was occurred from left to right, the meltwater penetrates into the remaining frost layer for about 45 mm. The water contents were analyzed in a 50 mm × 5 mm region (marked by yellow lines) by dividing into 20 sections in Fig.2. Defrosting process was started at t = 100 sec. At t = 140 sec, rapid meltwater penetration occurred by reaching the x = 45 mm position at t = 180 sec. The local water content reached at about 9 mg in x = 45 mm at t = 380 sec. As the temperature of the flat plate increases while keeping the temperature gradient, the meltwater moves to the right side of the plate. Hardly any residual water was observed on the plate.

REFERENCES:

[1] R. Matsumoto *et al.,* Transactions of the Japan Society of Refrigerating and Air Conditioning Engineers, **37(3)** (2020) 249.

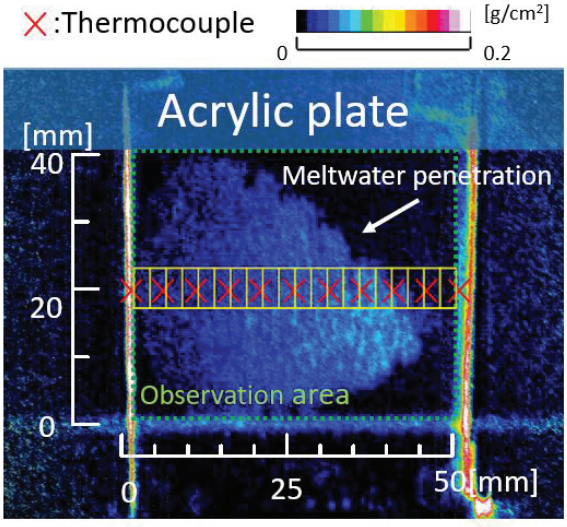

Fig. 1 Water penetration image.

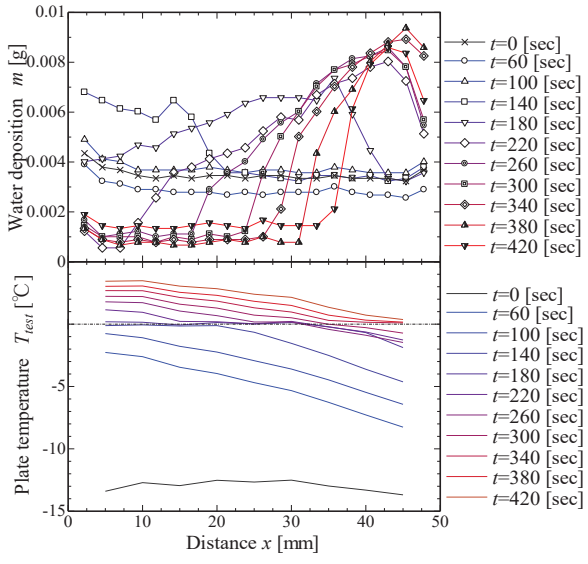

Fig. 2 Spatio-temporal distribution of meltwater penetration.

PR6-5

Spalling Phenomenon of High-Strength Concrete with Different Admixtures

K. Iwamura[1], M. Kanematsu[1], Y. Nishio[2], J. Kim[1], N. Odira[3], D. Ito[3] and Y. Saito[3]

[1]Department of Architecture, Tokyo University of Science
[2]Building Research Institute
[3]Institute for Integrated Radiation and Nuclear Science, Kyoto University

INTRODUCTION: Capturing detailed moisture movement in concrete under fire is essential to understanding the spalling mechanism [1]. In this study, using neutron radiography technology on high strength concrete with different admixtures, the effect of temperature and pressure changes and moisture movement inside the concrete during heating on the spalling phenomenon was examined.

EXPERIMENTS: 3 type concrete specimens (70×100×30 mm) with W / B of 18% are prepared. The first is general high-strength concrete(N), the second is N with replacing 40% blast furnace slag (BB) and the third is N with replacing rice husk ash (RHA). Temperatures and internal pressures were measured at the positions shown in Fig.1. In this experiment, specimens were heated from the bottom surface with quartz heater. Neutron radiography was performed at B-4 port of KUR.

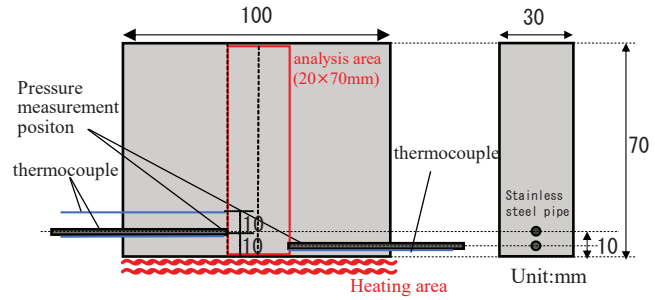

Fig. 1 Outline of concrete specimen

RESULTS: Fig. 2 and Fig. 3 show the result of a heating experiment with RHA. Fig. 2 shows the change in differential water intensity under heating, obtained by neutron radiography, and Fig. 3 shows the changes of temperature and pressure inside the concrete respectively. As shown in Fig. 2, areas with relatively high differential water intensity (dark blue areas) appeared at 5minutes. This trend was similar for the result with N and BB, which indicates forming moisture clog inside the concrete. As shown in Fig. 3, the maximum pressure was measured when the spalling occurred, and the measurement position was near the spalling depth. This suggests that the formation of water vapor pressure under heating affects the spalling occurrence. In the future, a more detailed investigation of the relationship between water vapor pressure and moisture clogs is expected

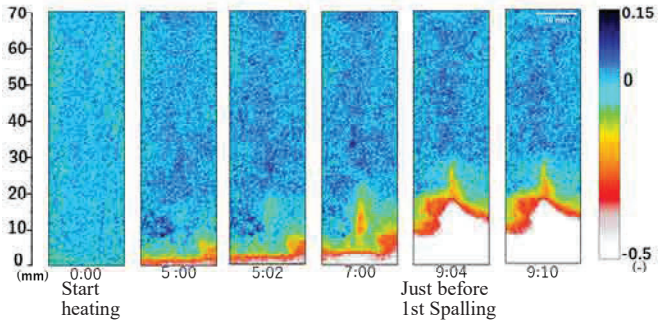

Fig. 2 Differential water intensity under heating (RHA)

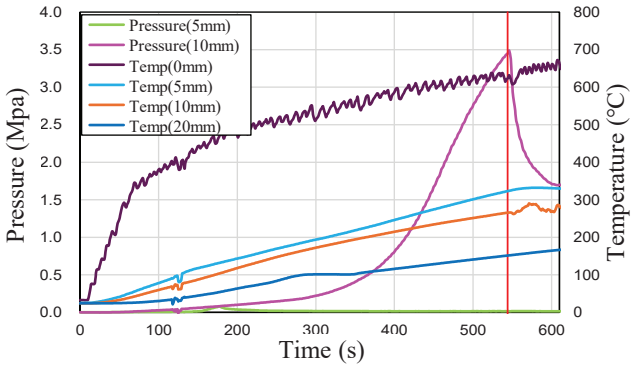

Fig. 3 Relationship between pressure and temperature in concrete under heating (RHA)

REFERENCES:

[1] JCI-TC-154A (2017). "Committee Reports:"
[2] T. Tanibe, (2014). "Ring restraining testing and spalling index of concrete at high temperature"

Neutron Radiography on a 1/16-inch Tee-Shaped Mixer with an Inner Diameter of 1.3 mm Used in Supercritical Hydrothermal Reactor

T. Kurono, S. Takami, Y. Azami[1], T. Saito[1], M. Kubo[1], K. Sugimoto[2], N. Odaira[3], D. Ito[3] and Y. Saito[3]

Graduate School of Engineering, Nagoya University
[1]Graduate School of Engineering, Tohoku University
[2]Graduate School of Engineering, Kobe University
[3]Institute for Integrated Radiation and Nuclear Science, Kyoto University

INTRODUCTION: Supercritical hydrothermal synthesis is a method to produce metal oxide nanoparticles in supercritical water. During supercritical hydrothermal synthesis using flow-type reactors, a stream of metal ion aqueous solution was instantaneously heated by mixing with a stream of supercritical water in a mixer. In the previous study, we visualized the mixing behavior of supercritical water and room temperature water in 1/8-inch and 1/4-inch tee-shaped mixers using neutron radiography. [1-3] We also found that a mixer with an inserted tube promoted faster mixing of reactant solutions with a stream of supercritical water.[4] In this study, we tried to visualize the mixing behavior at a tee-shaped mixer with an inner diameter of 1.3 mm.

EXPERIMENTS: In this study, we conducted neutron radiography measurements to visualize the mixing behavior in a flow-type reactor under operation. The measurements were performed at the B4 port of the Kyoto University Reactor (KUR). The KUR was operated at a 1 MW output with a neutron flux of ca. 1 or 5×10^7 n/cm^2 s at the beam exit of the B4 neutron guide tube. The experimental setup was similar to that used in previous studies.[1-4] The neutron beam that passed through the mixer was converted into fluorescent light using a 100 μm-thick ^{6}LiF/ZnS scintillator screen. A CMOS camera (ANDOR Zyla, 2048×2048 pixels) with a 180 mm telephoto lens (SIGMA APO MACRO DG HSM, f=3.5), a teleconverter (Nikon TC-201) and a close-up ring (Nikon PK-12) was used to capture the fluorescent light. The calculated spatial pixel resolution was around 13 μm. The distance between the neutron port and the converter was 2,310 mm

RESULTS: In this study, we tried to evaluate the mixing behavior of supercritical water and room temperature water in the 1/16-inch tee-shaped mixer with an inner diameter of 1.3 mm, which is expected to realize faster mixing. Due to the unexpected limitation of beam time availability, we were only able to visualize the mixer with room temperature water as shown in Fig. 1. As we can confirm, the room temperature water was precisely visualized using this setup. Therefore, we think the mixing behavior of supercritical water and room temperature water in 1/16 inch tee-mixer can be visualized using the similar setup.

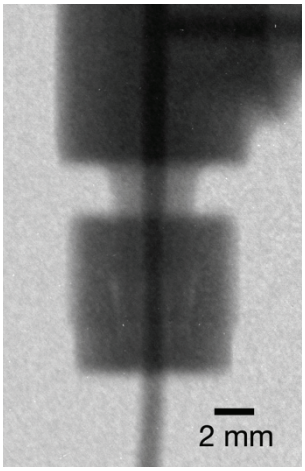

Fig. 1. Neutron radiography image of room temperature

REFERENCES:

[1] K. Sugioka *et al.,* AIChE J., **60** (2014) 1168-1175.
[2] S. Takami *et al.,* Phys. Proc., **69** (2015) 564-569.
[3] R. Sasaki *et al.,* J. Phys.: Conf. Ser., **2605** (2023) 012029.
[4] K. Sato *et al.,* Chem. React. Eng., **8** (2023) 1449-1456.

PR6-7

Visibility of Plant Roots in Different Artificial Soils via Neutron Imaging

U. Matsushima, O. Naoya[1], D. Ito[1], Y. Saitoh[1]

Faculty of Agriculture, Iwate University
[1]Institute for Integrated Radiation and Nuclear Science, Kyoto University, Japan

INTRODUCTION: This study compared the visibility of the root systems of plants cultivated in rice husks and perlite mixed media using neutron imaging.

EXPERIMENTS: *Brassica rapa* var. "perviridis" (Komatsuna) was the study material grown in rice husk (rice husks:soil = 3:1) and perlite mixed (perlite:soil = 9:1) media, in aluminum pots 14 × 14 × 14 mm. A thickness of 14 mm allowed neutrons to penetrate even wet media. The root system was observed using a neutron CT imaging device at the B4 beam hole, KUR, Kyoto University.

RESULTS: The rice husk medium, which contained organic matter, had low neutron permeability (Fig. 1-a), whereas perlite, which was mainly glassy with large grains and many voids, demonstrated high permeability (Fig. 1-b). In the peripheral region of the rice husk medium, roots developed well, root ball formation was apparent, and the root structure was confirmed. However, in the central part, the neutron permeability of the roots and the medium were similar, making it difficult to distinguish between them. As the neutron permeability in the perlite-mixed medium increased, the root visibility also improved. However, root development was inferior to that in the rice husk, and root identification in the central part of the medium was challenging. To observe plant root systems using neutron imaging, it is necessary to consider the neutron permeability and root development in the culture medium.

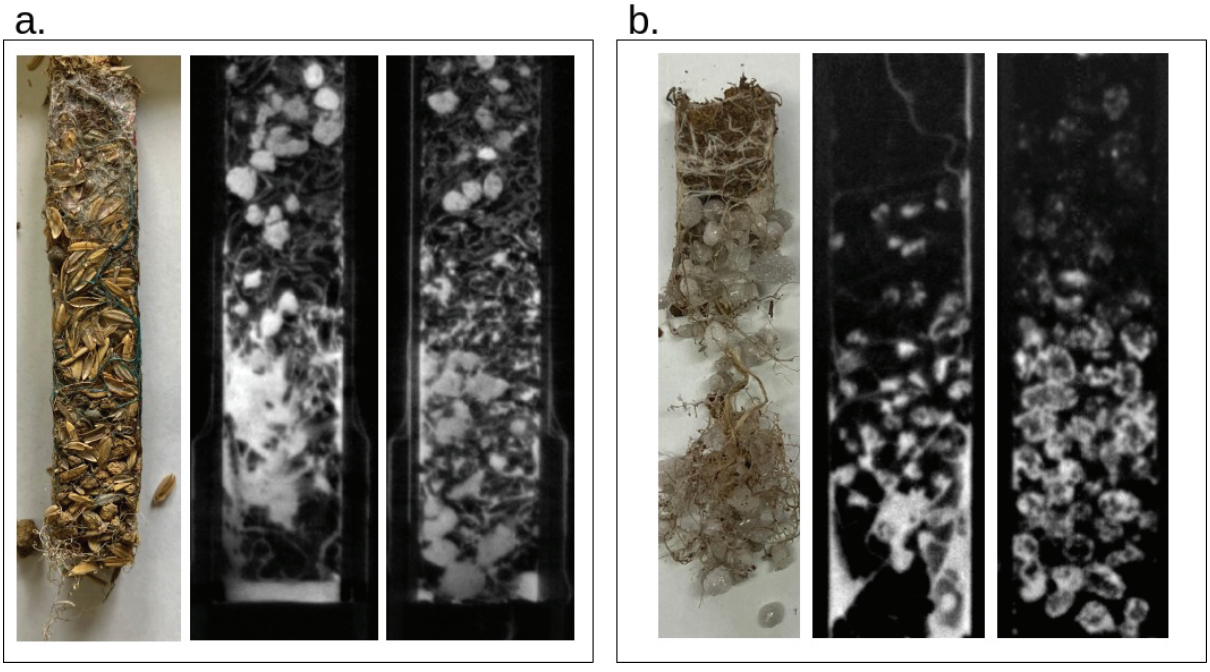

Fig. 1. Root systems of *Brassica rapa* var. "perviridis" (Komatsuna) grown in two culture medium and their neutron CT images.
From the left, root growth in the culture medium, and CT images of the peripheral and central areas of the culture medium. a. rice husks, b. perlite.

PR6-8

In-situ Observation of Lithium Migration in the Lithium-ion Conductor through Neutron Radiography under High-Temperature

S. Takai[1], H. Takagi[1], H. Ezaka[1], T. Yabutsuka[1], N. Odaira[2], D. Ito[2], and Y. Saito[2]

[1]*Graduate School of Energy Science, Kyoto University*
[2]*Institute for Integrated Radiation and Nuclear Science, Kyoto University*

INTRODUCTION: Lithium-ion migration in the solid electrolyte is the essential property for the operation of All-solid-state batteries. While the Li^+ ions migrate from the anode to the cathode through the electrolyte during battery operation, such behavior is hardly visualized due to the light element of lithium ions and the lack of appropriate radio isotopes. We have carried out the lithium diffusion coefficient measurement using the neutron radiography (NR) technique. We have measured the diffusion coefficient from the isotope profiles of the annealed samples by using the large difference in the neutron attenuation factors between ^{6}Li and ^{7}Li.

In the present study, we applied the electric field to the model cell to observe the lithium migration in the solid electrolyte employing the NR.

EXPERIMENTS: ^{7}Li-LAGP ($Li_{1.5}Al_{0.5}Ge_{1.5}(PO_4)_3$ using ^{7}Li) solid electrolyte and ^{6}Li-LMO ($LiMn_2O_4$ using ^{6}Li) electrode material were prepared by the conventional solid-state reaction method. A test cell consisting of Cu / ^{6}Li-LMO / PEO / ^{7}Li-LAGP / PEO / ^{6}Li-LMP / Al was constructed and electrolyzed at 300°C. Higher temperature operation than the previous (140°C) for the higher mobility of lithium ions. The mounted amount of cathode and anode materials are 3 and 6 mg, respectively. Before, after, and during the electrolysis, NR data were collected by CCD camera at the B4 guide tube in IIRNS, Kyoto University.

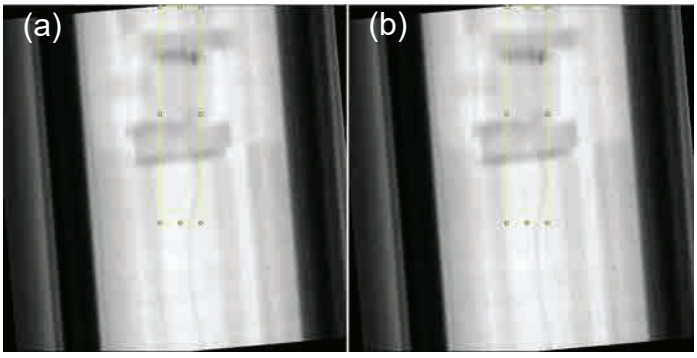

Fig. 1 NR images of test cell consisting of ^{7}Li-LAGP. (a) before and (b) after the electrolysis.

RESULTS: Fig. 1 shows the NR images of (a) before and (b) after the electrolysis. The ^{6}Li-containing part (electrode) in the test cell shows a darker image. The intermediate area between the electrodes corresponds to the LAGP electrolyte. Fig. 2 (a) shows the neutron-transmitted intensities of the image before and after the electrolysis. The divided data of (before) / (after) is represented in Fig. 2 (b). The electrolyte in the vicinity of the anode exhibits a little higher values, which indicate the introduction of ^{6}Li at the anode.

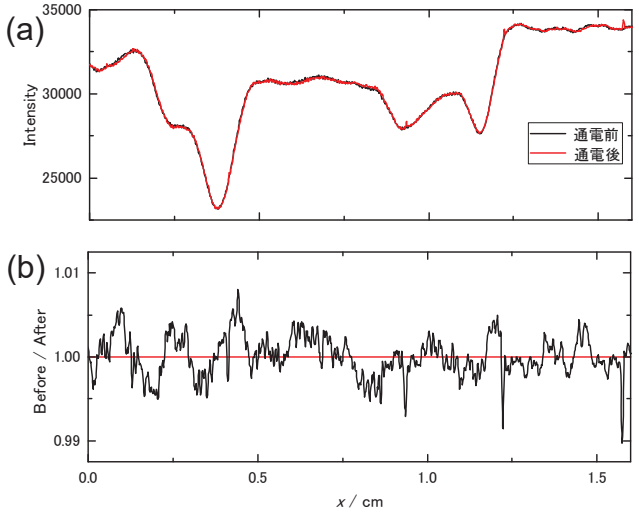

Fig. 2 (a) Neutron intensity profiles for the test cell before and after the electrolysis. (b) Division intensities of the cell.

PR6-9

Measurement of coolant distribution inside a flat laminate vapor chamber Utilizing neutron radiography

K. Mizuta, S. Shibata, Y. Saito[1], D. Ito[1]

Faculty of Engineering, Kagoshima University
[1]Institute for Integrated Radiation and Nuclear Science, Kyoto University

INTRODUCTION: Cooling electronic devices is becoming increasingly difficult due to rapid increase in performance and decrease in size of such devices, so more efficient cooling techniques are required to achieve sufficient reliability. We have been developing a flat laminate vapor cham-ber called FGHP(Fine Grid Heat Pipe) to contribute to tackle thermal problems in this field. In the previous studies, we found that FGHP has the highest thermal performance among various vapor chambers [1], and also found that thermal conductivity of FGHP in planar direction reached as high as 10,000 W m^{-1} K^{-1} at about 360 K [2]. Now we are developing larger size of FGHP than in the previous studies aiming at contributing wider range of applications. In this study, we tried to inves-tigate how the thermal performance of a newly developed FGHP changes with heat input and the change in coolant distribution with heat input by utilizing neutron radiography.

EXPERIMENTS: E-2 port of KUR was utilized for our experiments. Thermal neutron flux at the sample position was about $3x10^5$ cm^2s at 5MW operation. A test sample of FGHP utilized in this experiment was 100 mm square and 8 mm thick. The test sample was set vertically. A CCD camera (BU-53LN, BITRAN Co. Ltd., 4008×2672 pixels) and 6LiFZnS (50 μm thickness) were used. The effective spatial resolution was about 50 μm/pixel due to the scintillator screen characteristics. Neutron imaging of the sample was performed at the 1 MW operation mode and the exposure time was 300 s. Neutron images of the sample were utilized to calculate liquid thickness in the FGHP.

RESULTS: Fig 1 shows the variation of thermal resistance of the test sample with heat input and heater temperature, respectively. Circle key shows the data obtained through increasing heat input, and triangle key shows that obtained through decreasing heat input respectively. This figure shows that thermal resistance decreased with increasing heat input, which was the similar tendency found in our previous results [1]. Fig. 2 shows the variation of liquid thickness with heat input calculated at some points. From this figure, it was found that liquid thickness was almost constant regardless of heat input as found in our previous study [3], which means that the inner structure of a test sam-ple utilized in this study was still adequate enough for effective coolant circulation.

REFERENCES: [1] Mizuta, K., *et al.*, *Applied thermal management*, **104** (2016) 461-471. [2] Mizuta, K., *et al.*, *Ap-plied thermal management*, **146** (2019) 843-853.[3] Mizuta, K., *el al.*, *Physics Procedia*, **69** (2015) 556-563

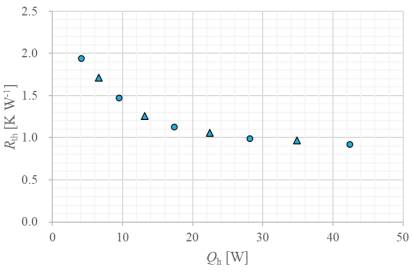

Fig. 1 Variation of thermal resistance with heat input.

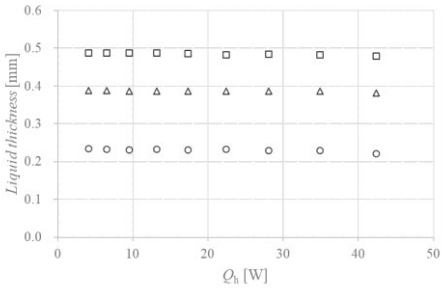

Fig. 2 Variation of liquid thickness of coolant with heater input.
(○:top, □:bottom, △:horizontal average)